

Time-property least-squares spectral method for population balance equations

C. A. Dorao · H. A. Jakobsen

Received: 17 December 2006 / Accepted: 30 September 2008 / Published online: 12 July 2009
© Springer Science+Business Media, LLC 2009

Abstract In multiphase chemical reactor analysis the dispersed phase distribution plays a major role in obtaining reliable predictions. The population balance equation is a well established equation for describing the evolution of the dispersed phase. However, the numerical solution of this type of equations is computationally intensive. In this work, a time-property least squares spectral method is presented for solving the population balance equation including breakage and coalescence processes. In this problem, both property and time are coupled in the least squares minimization procedure. Spectral convergence of the L^2 least squares functional and L^2 error norms in time-property is verified using a smooth solution to the population balance equation.

Keywords Population balance equation · Least squares method

1 Introduction

Population Balance Modeling (PBM) is a well established method for describing the evolution of populations of entities such as bubbles, droplets or particles. In particular, in multiphase flow problems the PBM is used to include information about the dispersed phase distribution into the multifluid model.

Based on the population balance approach the dispersed phase is treated by using a density function for instance $f(\mathbf{r}, \xi, t)$ where \mathbf{r} is the spatial vector position, ξ is the

C. A. Dorao

Department of Energy and Process Engineering, Norwegian University of Science and Technology,
7491 Trondheim, Norway

H. A. Jakobsen (✉)

Department of Chemical Engineering, Norwegian University of Science and Technology,
7491 Trondheim, Norway
e-mail: hugo.jakobsen@chemeng.ntnu.no

property of interest of the dispersed phase, and t the time. Thus, this density function $f(\mathbf{r}, \xi, t) d\xi$, can represent the average amount of number of particles per unit volume around the point \mathbf{r} at the instant t with the property between ξ and $\xi + d\xi$. The evolution of this density function must take into account the different processes that control the density function such as breakage, coalescence, growth and advective transport of the particles. The resulting equation is a nonlinear partial integro-differential equation which requires to be solved by a suitable numerical method.

Several methods have been proposed as reviewed by Ramkrishna [19] and Dorao and Jakobsen [5]. However, in order to introduce the population balance framework in computationally demanding environments such as in the simulation of bubble column reactors, high order methods might be a convenient option. In this respect, it is possible to find several examples of the application of high order methods for solving the population balance equation. For instance, Subramain and Ramkrishna [21] presented a Tau method for solving the distribution of the population of microbial cells that present growth and breakage processes. Mantzaris et al. [14] discussed the Galerkin, Tau and pseudo-spectral methods as a tool for solving multi-variable cell population balance models that present growth and breakage. Chen et al. [2] developed a wavelet-Galerkin method for solving population balance equations for the treatment of particle-size distribution in problems of a continuous, mixed-suspension and mixed-product removal crystallizer with effects of breakage. Liu and Cameron [12] proposed the use of a wavelet-based method for the treatment of problems involving particle nucleation, growth and agglomeration.

Recently, Dorao and Jakobsen [5,6] showed the applicability of the least squares method [1,11,16,17] using Legendre polynomials for the the particle space discretization and Crank–Nicolson for the time discretization. In particular, the least-squares finite element method constitutes an alternative to Galerkin and Petrov–Galerkin weak formulations. The basic idea in the least squares methods is to minimize the integral of the square of the residual over the computational domain. In the case when the exact solutions are sufficiently smooth the convergence rate is exponential. The population balance equation involving the advection operator for one-dimensional steady state problems were discussed by Dorao and Jakobsen [7] using a nodal approach. For problems involving spatial dependence Dorao and Jakobsen [8] presented the extension of the least squares method for including the spatial dependencies into the same minimization framework. For time dependent problems, the space-time formulation, i.e. time is treated as an additional dimension, allows high order accuracy both in space and in time [13,18]. In this way, space-time can be solved at once, or per time-step on a space-time slab in a kind of semi-discrete formulation.

The main goal of this work is to extend the least squares framework for solving the population balance equation previously developed [5–8] to include the time variation also in the minimization procedure, i.e. applying the time-property least squares approach. In this way, a balanced accuracy both in time and in space can be obtained.

In Sect. 2, the population balance equation is presented. Section 3 presents the application of the time-property least squares method for solving the population balance equation. In Sect. 4, some numerical examples are discussed. Finally, Sect. 5 presents the main conclusions of this work.

2 Population balance equation

The population balance equation can be written as

$$\mathcal{L}f(\xi, t) = g(\xi, t), \quad \text{in } \Omega \quad (1)$$

$$\mathcal{B}_0 f(\xi, t) = f_0(\xi), \quad \text{on } \Gamma_0 \quad (2)$$

with $\Omega = [\xi_{\min}, \xi_{\max}] \times [0, T]$ where ξ_{\min} and ξ_{\max} are for instance the minimum and maximum particle size, and T the final simulation time. The right hand side (RHS) of Eq. 1 is a source or sink term, representing an external mechanics of adding or removing particles from the system. Equation 2 contains the initial condition $f_0(\xi)$ of the problem which is applied on $\Gamma_0 = \{(\xi, t) \in \partial\Omega : t = 0\}$ and where \mathcal{B}_0 the identity operator, i.e. $\mathcal{B}_0 f(\xi, t) = f(\xi, t)$.

The operator \mathcal{L} is a non-linear first order partial integro-differential operator defined as

$$\mathcal{L}f(\xi, t) \equiv \frac{\partial f(\xi, t)}{\partial t} + \mathcal{L}_{PB}f(\xi, t) \quad (3)$$

where $\mathcal{L}_{PB}f(\xi, t)$ is, for this example, a 0th moment conservative population balance operator,

$$\begin{aligned} \mathcal{L}_{PB}f(\xi, t) = & -b(\xi)f(\xi, t) + \int_{\xi}^{\xi_{\max}} h(\xi, s)b(s)f(s, t)ds \\ & - f(\xi, t) \int_{\xi_{\min}}^{\xi_{\max} + \xi_{\min} - \xi} c(\xi, s)f(s, t)ds \\ & + \int_{\xi_{\min}}^{\xi} c(\xi - s, s)f(\xi - s, t)f(s, t)ds \end{aligned} \quad (4)$$

The first term on the RHS of Eq. 4 represents the change in the population due to loss of the individuals in the population for example for a breakage process; thus $b(\xi)$ is the *breakage rate* of the particles of type ξ . The second term on the RHS gives us the change in the population due to the arrivals of new individuals with property ξ . So, the breakage of particles of type s will produce particles of type ξ according to the *breakage yield function*, $h(\xi, s)$. Then, $h(\xi, s)$ satisfies the property that

$$h_k(s) = \int_{\xi_{\min}}^{\xi_{\max}} \xi^k h(\xi, s) d\xi = s^k \quad (5)$$

where $h_k(s)$ is the moment of the new particles that appear after the breakage, if k is the moment that is conserved in the breakage process. For instance, assuming that ξ represents the volume of the particle: if the sum of the volume of the particles that appears due to the breakage of a particle with volume s is conserved, then we have that $k = 1$, i.e. the 1th moment is conserved.

The third term on the RHS of Eq. 4 represents the change in the population due to the loss of individuals due to pair interactions such as a coalescence process. Thus, $c(\xi, s)$ is the *coalescence rate* between particles of type ξ and s . It is important to remark that the upper limit of the integral is defined such that the coalescence process can not produce particles exceeding the maximum physical allowable size ξ_{\max} . The fourth term on the RHS represents the arrivals of new individuals due to the pair interaction, one particle of type ξ_1 that coalesces with a particle of type ξ_2 will produce a particle of type $\xi = \xi_1 + \xi_2$. Depending on the property ξ chosen, the previous relationships should be modified accordingly.

Further discussion about the meaning of each term in Eq. 4 regarding the modeling of bubble flows can be found in Jakobsen et al. [10].

3 The least squares method

The least squares method (LSM) is a well established numerical method for solving a wide range of mathematical problems, (e.g. [1, 11, 16, 17]). The basic idea in the LSM is to minimize the integral of the square of the residual over the computational domain. In the case when the exact solutions are sufficiently smooth the convergence rate is exponential. For time dependent problems, the space-time formulation, i.e. time is treated as an additional dimension, allows high order accuracy both in space and in time (e.g. [13, 18]). In this way, space-time can be solved at once, or per time-step on a space-time slab in a kind of semi-discrete formulation. A comprehensive discussion of the LSM for a wide range of applications, and its mathematical properties have been examined by Bochev [1]; Jiang [11]. Besides, an extended discussion about the advantages of the time-space least squares can be found in Potanza and Reddy (e.g. [18]). For application examples of the LSM to integral equations like the Fredholm, Volterra or integro-differential equations the interested reader is referred to Delves and Mohamed [3] and Hackbush [9]. In particular, the application of LSM to PBE was previously discussed by Dorao and Jakobsen [5, 6].

The Least-Squares formulation is based on the minimization of a norm-equivalent functional. This consists in finding the minimizer of the residual in a certain norm. The norm-equivalent functional is given by

$$\mathcal{J}(f; g, f_0) \equiv \frac{1}{2} \| \mathcal{L}f - g \|_{Y(\Omega)}^2 + \frac{1}{2} \| \mathcal{B}_0 f - f_0 \|_{Y(\Gamma_0)}^2$$

with the norms defined like

$$\| \bullet \|_{Y(\Omega)}^2 = \langle \bullet, \bullet \rangle_{Y(\Omega)} = \int_{\Omega} \bullet \bullet \, d\Omega, \tag{6}$$

$$\| \bullet \|_{Y(\Gamma_0)}^2 = \langle \bullet, \bullet \rangle_{Y(\Gamma_0)} = \int_{\Gamma_0} \bullet \bullet \, ds \tag{7}$$

Based on variational analysis, the minimization statement is equivalent to:

Find $f \in X(\Omega)$ such that

$$\lim_{\epsilon \rightarrow 0} \frac{d}{d\epsilon} \mathcal{J}(f + \epsilon v; g, f_0) = 0 \quad \forall v \in X(\Omega) \tag{8}$$

where $X(\Omega)$ is the space of the admissible functions. Consequently, the necessary condition can be written as:

Find $f \in X(\Omega)$ such that

$$\mathcal{A}(f, v) = \mathcal{F}(v) \quad \forall v \in X(\Omega) \tag{9}$$

with

$$\mathcal{A}(f, v) = \langle \mathcal{L}f, \mathcal{L}v \rangle_{Y(\Omega)} + \langle \mathcal{B}_0 f, \mathcal{B}_0 v \rangle_{Y(\Gamma_0)} \tag{10}$$

$$\mathcal{F}(v) = \langle g, \mathcal{L}v \rangle_{Y(\Omega)} + \langle f_0, \mathcal{B}_0 v \rangle_{Y(\Gamma_0)} \tag{11}$$

where $\mathcal{A} : X \times X \rightarrow \mathbb{R}$ is a symmetric, continuous bilinear form, and $\mathcal{F} : X \rightarrow \mathbb{R}$ a continuous linear form. Finally, the discretization statement consists in searching the solution in a reduced subspace, i.e. $f_N(r, \xi) \in X_N(\Omega) \subset X(\Omega)$. Hence, f_N can be expressed like

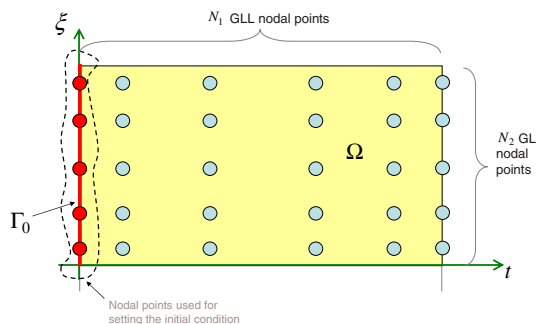
$$f_N(\xi, t) = \sum_{i=0}^{N_1} \sum_{j=0}^{N_2} f_{ij} \varphi_i(\xi) \varphi_j(t), \quad \text{with } f_{ij} = f(\xi_i, t_j) \tag{12}$$

where $\varphi_i(\xi)$ and $\varphi_j(t)$ are the one dimensional basis functions. These basis functions consist of Lagrangian interpolants polynomials through the Gauss–Legendre (GL) and Gauss–Lobatto–Legendre (GLL) collocation points, respectively. For example the polynomial $\varphi_j(t)$ defined in the reference domain $\hat{\Omega} = [-1, 1]$ is given by

$$\varphi_j(t) = \frac{(\xi^2 - 1) \frac{dL_{N_2}(\xi)}{d\xi}}{N_2(N_2 + 1)L_{N_2}(\xi)(\xi - \xi_j)} \tag{13}$$

where the $(N_2 + 1)$ GLL–points, ξ_j , are the roots of the first derivative of the Legendre polynomial of degree N_2 , extended with the boundary nodes [4]. Figure 1 shows an example of the distribution of nodal GLL and GL points in the domain Ω and in the initial boundary Γ .

Fig. 1 Nodal points for the time-property discretization



Defining the index $l = i + j(N_1 + 1)$ with $0 \leq i \leq N_1$ and $0 \leq j \leq N_2$, and $\mathcal{N} = (N_1 + 1)(N_2 + 1) - 1$, as it can be seen in Fig. 2, expression (12) can be written as

$$f_N(\mathbf{x}) = \sum_{l=0}^{\mathcal{N}} f_l \Phi_l(\mathbf{x}), \quad \text{with } f_l = f(\mathbf{x}_l) \tag{14}$$

with $\mathbf{x} = (\xi, t)$ and $\Phi_l(\mathbf{x}) = \varphi_j(t) \varphi_i(\xi)$ a two-dimensional basis function defined as the tensor product of two one-dimensional basis functions. Figure 3 shows one example of one two-dimensional basis function $\Phi_l(\mathbf{x})$.

Using the approximation (14) in expression (9), the following matrix system is obtained

$$\mathcal{A} f = \mathcal{F} \tag{15}$$

Fig. 2 The distribution of the GLL–GL points, \mathbf{x}_i , in $[-1, 1]^2$

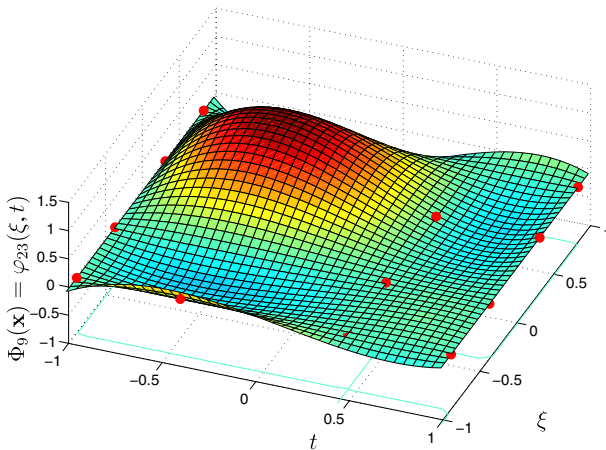
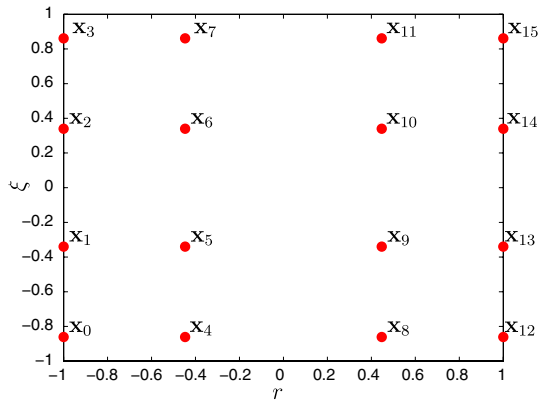


Fig. 3 One of the 16 basis functions $\Phi_l(\mathbf{x}) = \varphi_{ij}(\xi, t)$ in $[-1, 1]^2$

where the matrix $\mathcal{A} \in \mathbb{R}^{\mathcal{N} \times \mathcal{N}}$ and vectors $\mathbf{f}, \mathcal{F} \in \mathbb{R}^{\mathcal{N}}$ are defined like

$$[\mathcal{A}]_{ij} = \mathcal{A}(\Phi_j, \Phi_i) = \langle \mathcal{L}\Phi_j, \mathcal{L}\Phi_i \rangle_{Y(\Omega)} + \langle \mathcal{B}_0\Phi_j, \mathcal{B}_0\Phi_i \rangle_{Y(\Gamma_I)} \quad (16)$$

$$[\mathcal{F}]_i = \mathcal{F}(\Phi_i) = \langle g, \mathcal{L}\Phi_i \rangle_{Y(\Omega)} + \langle f_I, \mathcal{B}_0\Phi_i \rangle_{Y(\Gamma_I)} \quad (17)$$

$$[\mathbf{f}]_i = f_i = f(\mathbf{x}_i) \quad (18)$$

with

$$\langle \mathcal{L}\Phi_j, \mathcal{L}\Phi_i \rangle_{Y(\Omega)} = \int_0^T \int_{\xi_{\min}}^{\xi_{\max}} \mathcal{L}\Phi_j(\xi, t) \mathcal{L}\Phi_i(\xi, t) d\xi dt \quad (19)$$

$$\langle \mathcal{B}_0\Phi_j, \mathcal{B}_0\Phi_i \rangle_{Y(\Gamma_0)} = \int_0^T \mathcal{B}_0\Phi_j(\xi, t) \mathcal{B}_0\Phi_i(\xi, t) d\xi \quad (20)$$

$$\langle g, \mathcal{L}\Phi_i \rangle_{Y(\Omega)} = \int_0^T \int_{\xi_{\min}}^{\xi_{\max}} g(\xi, t) \mathcal{L}\Phi_i(\xi, t) d\xi dt \quad (21)$$

$$\langle f_0, \mathcal{B}_0\Phi_i \rangle_{Y(\Gamma_0)} = \int_0^T f_0(\xi) \mathcal{B}_0\Phi_i(\xi, 0) d\xi \quad (22)$$

The previous integral expressions can be approximated in an efficient way by using numerical quadrature [4]. For example, the integral of a function $b(\xi)$ in the reference domain $\hat{\Omega} = [-1, 1]$ evaluated numerically using GL integration is given as

$$\int_{-1}^1 b(\xi) d\xi \approx \sum_{q=0}^P b(\xi_q) w_q \quad (23)$$

Generally, the same GL-roots are used for the evaluation of the integrals as for the approximation of the solution, i.e. $P = N_1$, because of simplicity and for the implementation aspects. The Gaussian quadrature based on the GL-roots is even exact when the integrand $b(\xi)$ is a polynomial of degree $2P - 1$ or lower. Thus, it is possible to determine a priori for a given problem the optimal order of P .

It is important to mention that the non-linear terms require a linearization step before the application of the framework discussed in Dorao and Jakobsen [5], where the successive approximation linearisation method was used.

3.1 Further extensions

The novel framework is not limited to the particular case discussed in this work where the density function $f(\xi, t)$ is only dependent on one particle property. The extension for considering more particle properties and/or spatial dependency is also possible using the same mathematical framework. Increasing the number of dimensions requires that one increases the dimension of the space $X_N(\Omega)$. Hence, approximation (12) should include the one-dimensional basis functions related to the considered dimensions.

4 Numerical example

In order to verify the spectral convergence of this framework, the method of manufactured solutions is used [15,20]. The method of manufactured solutions consists in proposing an analytical solution, preferably one that is infinitely differentiable and not trivially reproduced by the basis functions of the approximation, and the produced residuals are simply treated as source terms that produce the desired or prescribed solution. This source terms or residuals are referred to as the *consistent forcing functions*.

The test case is defined like

$$\begin{aligned}
 b(\xi) &= \xi^2, \quad h(\xi, \tilde{\xi}) = 1/\tilde{\xi}, \quad c(\xi, \tilde{\xi}) = 1 \\
 g(\xi, t) &= \frac{1}{12} e^{-2-2t-2\xi} (15e^{t+2\xi} + 3e^{2\xi} \xi(-3 + 2\xi) \\
 &\quad + e^2 (3\xi - 2\xi^3) + 3e^{2+t}(-1 - 6\xi - 2\xi^2 + 4\xi^3)) \\
 f_{\text{exact}}(\xi, t) &= \xi e^{-2\xi-t}
 \end{aligned}$$

where $(\xi, t) \in \Omega = [0, 1] \times [0, T]$.

The integration computations, expressions (19) to (22), required for getting the final system and errors estimates are computed using a GL–GLL quadrature rule of the same order as the used for the Lagrangian polynomials.

The solution is approximated on successive space-time strips of dimensions $\Omega_t = [0, 1] \times \Delta t$. Within each space-time slab the problem is solved iteratively until convergence is reached

$$|\Delta R| \leq \text{tol}, \quad \text{with } \Delta R = \| R(f_N^i) \|_{L^2} - \| R(f_N^{i+1}) \|_{L^2} \tag{24}$$

where $\text{tol} = 10^{-14}$, f_N^i and f_N^{i+1} are the approximated solution in two successive iterations. The residual $\| R \|_{L^2}$ is in the L^2 -norm

$$\| R \|_{L^2} = \left(\| \mathcal{L}f_N - g \|_{Y(\Omega)}^2 + \| f_N - f_0 \|_{Y(\Gamma_0)}^2 \right)^{1/2} \tag{25}$$

In order to show how good the numerical solutions of the above problems are in comparison with the exact ones, the error over the total time-space domain Ω are computed and measured in the L^2 -norm

$$\| \epsilon \|_2 = \left(\int_0^T \int_0^1 (f(\xi, t) - f_N(\xi, t))^2 d\xi dt \right)^{1/2} \tag{26}$$

where $f(\xi, t)$ is the exact solution and $f_N(\xi, t)$ is the LSQ solution. In some practical applications, the prediction of the moments is the main goal of the computations. For

that reason, for showing how accurate the moments are computed, the error in the weighted L^1 -norm is used

$$\| \epsilon_k(t) \|_1 = 100 \left| \frac{\mu_k(t) - \mu_{k,N}(t)}{\mu_k(t)} \right| \tag{27}$$

where $\mu_k(t)$ and $\mu_{k,N}(t)$ are the exact and numerical moments, respectively. It is noted that the moments are defined as

$$\mu_k(t) = \int_0^1 \xi^k f(\xi, t) d\xi \tag{28}$$

Figure 4 shows the error and residual convergence in the L^2 -norm. As expected, the exponential convergence rate is observed. In some engineering applications, the accurate prediction of the moments is the main goal of the computations. For that reason, in Fig. 5 the convergence error in the moments is plotted.

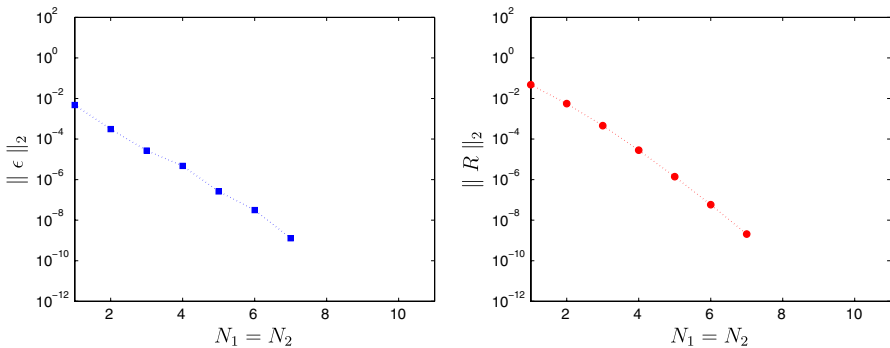
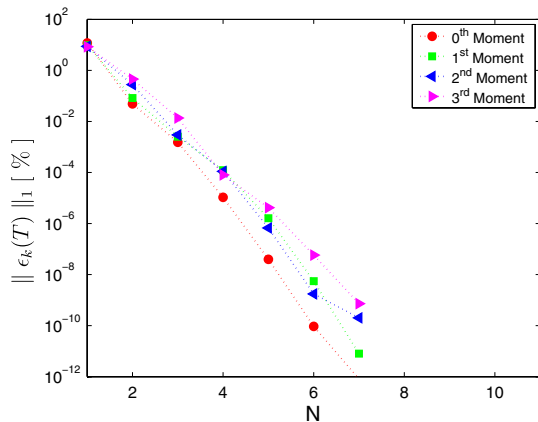


Fig. 4 Error and Residual convergence in the L^2 -norm, with $\Omega = [0, 1]^2$ and $\Delta t = 1$

Fig. 5 Moments error convergence in the L^1 -norm, with $\Omega = [0, 1]^2$ and $\Delta t = 1$



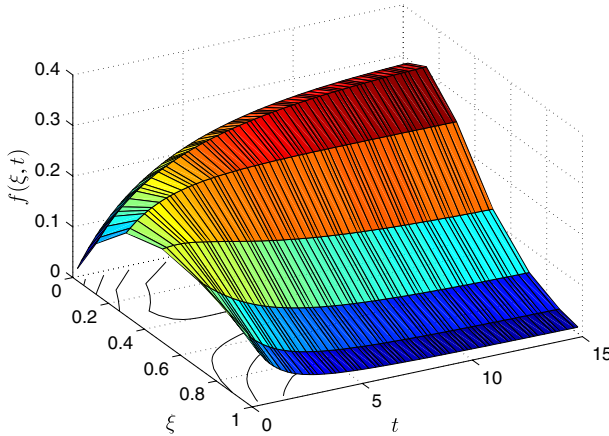
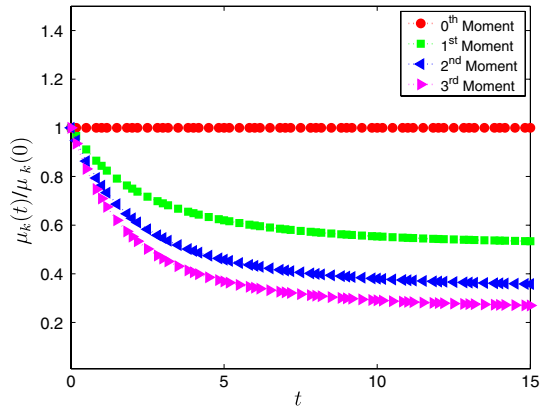


Fig. 6 Evolution of $f(\xi, t)$ with $N_1 = 6, N_2 = 4, \Omega = [0, 1]^2, \Delta t = 0.1, \|R\|_2 = 6.0 \times 10^{-6}$

Fig. 7 Evolution of the normalized moments with $N_1 = 6, N_2 = 4, \Omega = [0, 1]^2, \Delta t = 0.1$ and $\|R\|_2 = 6.0 \times 10^{-6}$



In Fig. 6 the evolution of $f(\xi, t)$ is plotted for the case that $g(\xi, t) = 0$, for which no analytical solution is available. Besides, Fig. 7 shows the time evolution of the normalized moments for the same case. In particular, the 0th moment is conserved.

5 Conclusions

A time-property least squares spectral method was presented for solving the population balance equation including breakage and coalescence processes. The use of a time-property approach allows us to increase the temporal accuracy or for a given accuracy increase the time step reducing the final computational cost. Besides, if the exact solution is sufficiently smooth, the convergence rate is exponential.

Further work is required for coupling such type of methods with the available multifluid solvers.

Acknowledgements The PhD fellowship (Dorao, C. A.) financed by the Research Council of Norway through a Strategic University Program (CARPET) is gratefully appreciated.

References

1. P. Bochev, *Finite element methods based on least-squares and modified variational principles*, Technical report, POSTECH (2001)
2. M. Chen, C. Hwang, Y. Shih, A wavelet-galerkin method for solving population balance equations. *Comp. Chem. Eng.* **20**(2), 131–145 (1996)
3. L.M. Delves, J.L. Mohamed, *Computational methods for integral equations* (Cambridge University Press, London, 1985)
4. M.O. Deville, P.F. Fischer, E.H. Mund, *High-order methods for incompressible fluid flow* (Cambridge University Press, Cambridge, 2002)
5. C.A. Dorao, H.A. Jakobsen, Application of the least square method to population balance problems. *Comp. Chem. Eng.* **30**(3), 535–547 (2005)
6. C.A. Dorao, H.A. Jakobsen, An evaluation of selected numerical methods for solving the population balance equation. Fourth International Conference on CFD in the Oil and Gas, Metallurgical & Process Industries. (SINTEF/NTNU Trondheim, Norway, 2005), 6–8 June 2005
7. C.A. Dorao, H.A. Jakobsen, Application of the least squares method for solving population balance problems in \mathbb{R}^{d+1} . *Chem. Eng. Sci.* **61**(15), 5070–5081 (2005)
8. C.A. Dorao, H.A. Jakobsen, A least squares method for solving advective population balance problems. *J. Comp. Appl. Math.* **201**(1), 247–257 (2005).
9. W. Hackbusch, *Integral equation: theory and numerical treatment. International series of numerical mathematics*, vol. 120 (Birkhauser Verlag, Basel, 1995)
10. H.A. Jakobsen, H. Lindborg, C.A. Dorao, Modeling of bubble column reactors: progress and limitations. *Ind. Eng. Chem. Res.* **44**(14), 5107–5151 (2005)
11. B. Jiang, *The least-square finite element method: theory and applications in computational fluid dynamics and electromagnetics* (Springer, New York, 1998)
12. Y. Liu, T. Cameron, A new wavelet-based method for the solution of the population balance equation. *Chem. Eng. Sci.* **56**, 5283–5294 (2001)
13. De Maerschalck B. (2003) *Space-Time least-squares spectral element method for unsteady flows - application and evaluation for linear and non-linear hyperbolic scalar equations*, Master Thesis Report, Delft University of Technology, Dept. of Aerospace Engineering, The Netherlands, 2003
14. N.V. Mantzaris, P. Daoutidis, F. Srienc, Numerical solution of multi-variable cell population balance models. II. Spectral methods. *Comp. Chem. Eng.* **25**, 1441–1462 (2001)
15. D. Post, R. Kendall, Software project management and quality engineering practices for complex, coupled multi-physics, massively parallel computational simulations: lessons learned from ASCI. *Int. J. High Perform. Comp. Appl.* **18**(4), 399–416 (2003)
16. M.M.J. Proot, M.I. Gerritsma, A least-squares spectral element formulation for stokes problem. *J. Sci. Comp.* **17**(1–4), 285–296 (2002)
17. J.P. Pontaza, J.N. Reddy (2004) Spectral/hp least-squares finite element formulation for the incompressible Navier–Stokes equation. *J. Comput. Phys.* **190**(2), 523–549 (2003)
18. J.P. Pontaza, J.N. Reddy, Space-time coupled spectral/hp least squares finite element formulation for the incompressible Navier–Stokes equation. *J. Comput. Phys.* **190**(2), 418–459 (2004)
19. D. Ramkrishna, *Population balances, theory and applications to particulate systems in engineering* (Academic Press, San Diego, 2000)
20. C.J. Roy, Review of code and solution verification procedures for computational simulation. *J. Comput. Phys.* **205**, 131–156 (2005)
21. G. Subramain, D. Ramkrishna, On the solution of statistical models of cell populations. *Math. Biosci.* **10**, 1–23 (1971)